Clays and Clay Minerals, Vol. 45, No. 2, 132–146, 1997.

DECOMPOSITION OF EXPERIMENTAL X-RAY DIFFRACTION PATTERNS (PROFILE FITTING): A CONVENIENT WAY TO STUDY CLAY MINERALS

BRUNO LANSON

Environmental Geochemistry Group, LGIT IRIGM, University of Grenoble and CNRS, BP 53, 38041 Grenoble Cedex 9, France

Abstract—This paper thoroughly describes the decomposition procedure, using the example of DECOMPXR (Lanson 1990). The steps of the decomposition procedure are: 1) preliminary data processing; 2) decomposition; 3) validation of results; and 4) use of the results. The use of decomposition is restricted to the separation of contributions from various phases. The effect of preliminary data processing steps (data smoothing, background stripping) on profile shape is shown to be limited and their implementation is detailed. Potential experimental limitations such as peak symmetry, experimental reproducibility or discrimination are equally minor. A logical decomposition process starts from the definition of the angular range to be fitted, proceeds with the determination of the number of elementary peaks to be fitted and ends with the check for results consistency.

Numerical data processing is a powerful tool for the accurate identification of monophases, because of the additional parameters available to constrain XRD profile simulation. Ultimately, however, the match over the whole angular range of both the experimental and the simulated patterns remains the only valid way to characterize the phases present in the sample. Additionally, the decomposition procedure permits both the identification of complex clay mineral assemblages and the characterization of their evolution. This step constrains, and may help to determine, the reaction mechanisms of a transformation; and, as a consequence, to characterize and to model the kinetics of this transformation.

Key Words—Clay Minerals, Decomposition, Mixed Layering, Simulation, X-ray Powder Diffraction.

INTRODUCTION

The recent availability of both computer-driven diffractometers and increasingly powerful computers has enabled development of data processing routines to obtain more information from an XRD profile. For example, a decomposition routine is now widely used to separate the respective contributions of partially overlapping peaks due to phases with distinct but closely related crystallographic characteristics from a complex XRD profile (Howard and Preston 1989; Jones 1989; Lanson and Champion 1991; Righi and Meunier 1991; Stern et al. 1991; Bouchet et al. 1992; Lanson and Besson 1992; Drits et al. 1993; Robinson and Bevins 1994; Renac and Meunier 1995; Righi et al. 1995; Lanson et al. 1996). In this paper, the word "phase" describes a population of particles whose characteristics (such as size or chemical composition) vary about a mean value. It is assumed that this population behaves as a single phase (in a thermodynamic sense) having the same mean characteristics. Consequently, the word is used herein in the thermodynamic sense.

Such a decomposition routine is especially useful because the inability to separate the contributions from different phases often impairs their identification. Even though the trial-and-error crystallographic simulation approach (Drits et al. 1990) may be used to model complex polyphasic XRD profiles (Lanson and Besson 1992), it is too time-consuming for routine application to dozens of samples. For any phase in a sample, a decomposition routine can provide information such as peak position, full width at half maximum intensity (FWHM), relative intensities or profile shape. These data help to efficiently constrain the large number of adjustable parameters for the simulation process, which remains the only valid way to accurately identify these phases using XRD. Such information is even more relevant when the user is aware of routines' limitations. It is useful to know whether any simplifying hypotheses (such as convergence criteria) have been used while developing the algorithm and what possible effects they could have on the reproducibility of results. Decomposition routines are iterative procedures. The quality of the fit is estimated after each iteration, as well as the evolution of the adjusted parameters. The calculation is stopped when the quality of the fit is not improving and/or when adjusted parameters are stable. The "convergence criteria" are arbitrarily defined limits of the "stability" domain of both the quality of fit and adjusted parameters. These effects may be emphasized when working on clay minerals, because commercially available numerical treatment packages are often designed to deal with well-crystallized phases. On the contrary, clay mineral diffraction peaks are usually broad and widely overlapping. These specific characteristics result in diffraction profiles showing a very slow variation of their first derivative as well as a very poor peak separation.

Copyright © 1997, The Clay Minerals Society

https://doi.org/10.1346/CCMN.1997.0450202 Published online by Cambridge University Press

A decomposition routine provides the user with more reproducible information out of the same XRD patterns. The numerical treatment cannot replace collection of the various diffractograms necessary for an unequivocal identification of clay phases. This method is fast (from 10 s to a few min for the processing of 1 complex band) and powerful; however, one must check the decomposition results both over the whole angular range and against other analytical data from the sample (Lanson and Besson 1992; Lanson and Velde 1992). The decomposition procedure may be used to characterize any clay assemblage, and is especially useful for complex ones such as those from soils (Righi and Meunier 1991; Righi et al. 1993; Righi et al. 1995). It is also suitable for the study of relative variation within a series of samples whose compositions lie between identified end members (Lanson and Champion 1991; Lanson and Besson 1992; Renac and Meunier 1995; Varajao and Meunier 1995; Lanson et al. 1995).

This paper describes the decomposition procedure using the example of the DECOMPXR code (Lanson 1990). The simulation process used to identify XRD characteristics of the various phases characterized by decomposition is described by Lanson and Champion (1991) and Lanson and Velde (1992). Application of the decomposition method is restricted to the separation of the contributions from various phases to the diffracted intensity, whereas it is possible with the deconvolution procedure to extract the pure diffraction profile and the instrumental contribution from an experimental XRD profile. The effect on profile shape of preliminary data processing steps (data smoothing, background stripping) is detailed. Experimental limitations such as peak symmetry, experimental reproducibility and discrimination are discussed. A standard decomposition procedure is proposed and its logic detailed. Because of its essential character, special attention is given to determining the number of elementary peaks to be fitted. Precise criteria and constraints are given to check the results consistency. Finally, application of numerical data processing to the identification of single-phase samples, and the description of both complex clay assemblages and their evolution are illustrated in the context of late-stage diagenesis (illitic material) and hydrothermal systems (chloritic mixed layers).

DECOMPOSITION VERSUS DECONVOLUTION

The difference between "deconvolution" and "decomposition" (Jones 1989) is not well understood by many. The XRD profile of a polyphase sample is the sum of the contributions from various phases. If $A(\theta)$ and $B(\theta)$ are the intensity profiles of these 2 phases, the total intensity is:

$$I(\theta) = A(\theta) + B(\theta) \quad [1]$$

Elementary contributions from each phase are the convolution of 3 components: the diffraction profile of the phase, the geometrical aberrations of the instrument and the emission profile of the radiation. If $f(\theta)$ is the diffraction profile of the specimen and $g(\theta)$ is the instrumental signature, convolution of the geometrical instrumental aberrations and of the emission profile of the radiation, the total intensity is:

$$I(\theta) = \int_{-\infty}^{+\infty} g(x) \cdot f(\theta - x)\, dx \quad [2]$$

To obtain the global XRD profile, it is equivalent to add all elementary contributions after convolution by the instrumental signature, or to perform the convolution operation of the instrumental signature with the sum of pure diffraction profiles from all phases.

The decomposition procedure can be used to fit an experimental XRD pattern with several elementary curves assumed to represent the respective contributions from the various phases to the total profile. Alternatively, the deconvolution procedure can be applied to the diffraction profile of a single phase to obtain its pure line profile. The convolution of the geometrical aberrations and of the emission profile of the radiation must be determined experimentally by using a standard specimen with the same chemical composition as the unknown, and negligible diffraction broadening. For example, this deconvolution procedure is the first step of the Warren-Averbach method which is used to determine the coherent scattering domain size of the sample along specific crystallographic directions. It is the only way to separate the instrumental and sample contributions.

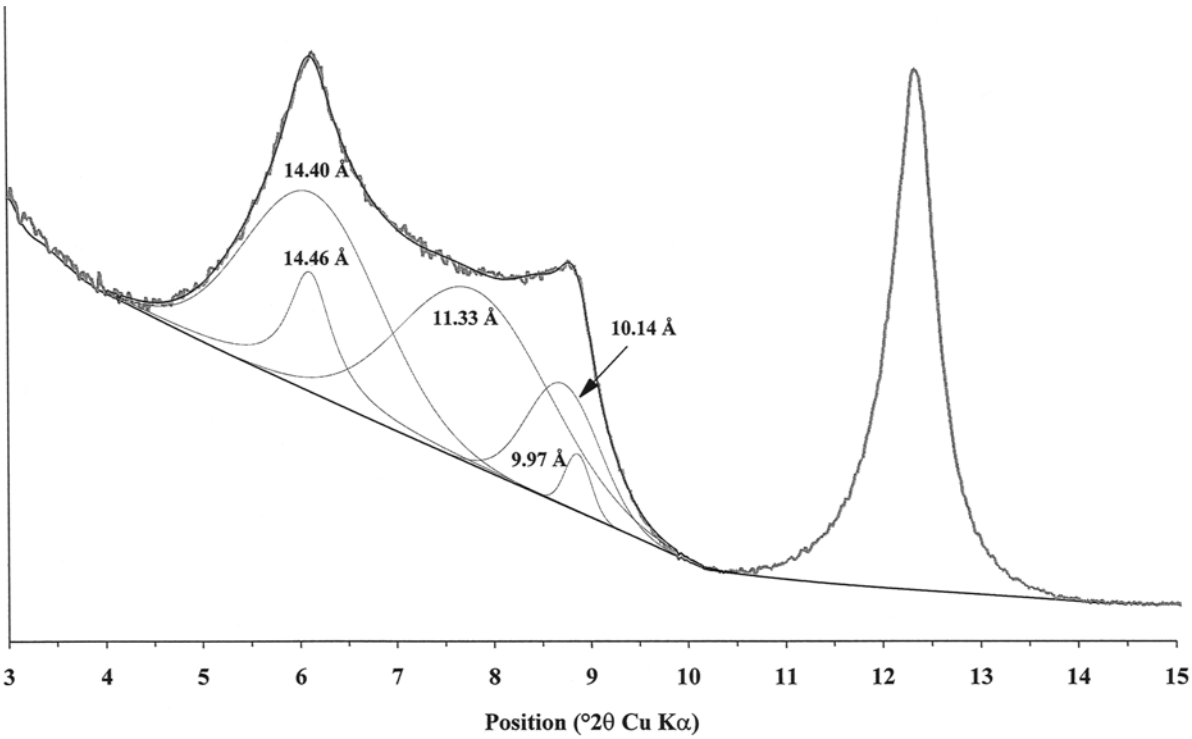
PRELIMINARY DATA PROCESSING

Before a decomposition procedure can be used, numerical data must be collected. Then preliminary data filtering may be necessary to enhance experimental data quality. Background stripping must be introduced if the background is not fitted simultaneously with the sample contribution, which is the case with DECOMPXR.

Experimental Data Filtering

The low noise of the modern powder diffractometer induces few electronic "pulses"; however, elimination of aberrant data points may still be useful for older diffraction systems updated with a computer-driven motor control and data collection system. There are 2 methods for detecting such aberrant data points: numerical (systematic comparison with the neighboring data points and definition of a criterion for discarding) or manual (in which the user's eye plays the detector role). Such points can either be removed or their intensity can be corrected. Using DECOMPXR, aberrant data are replaced rather than disregarded, because the

https://doi.org/10.1346/CCMN.1997.0450202 Published online by Cambridge University Press



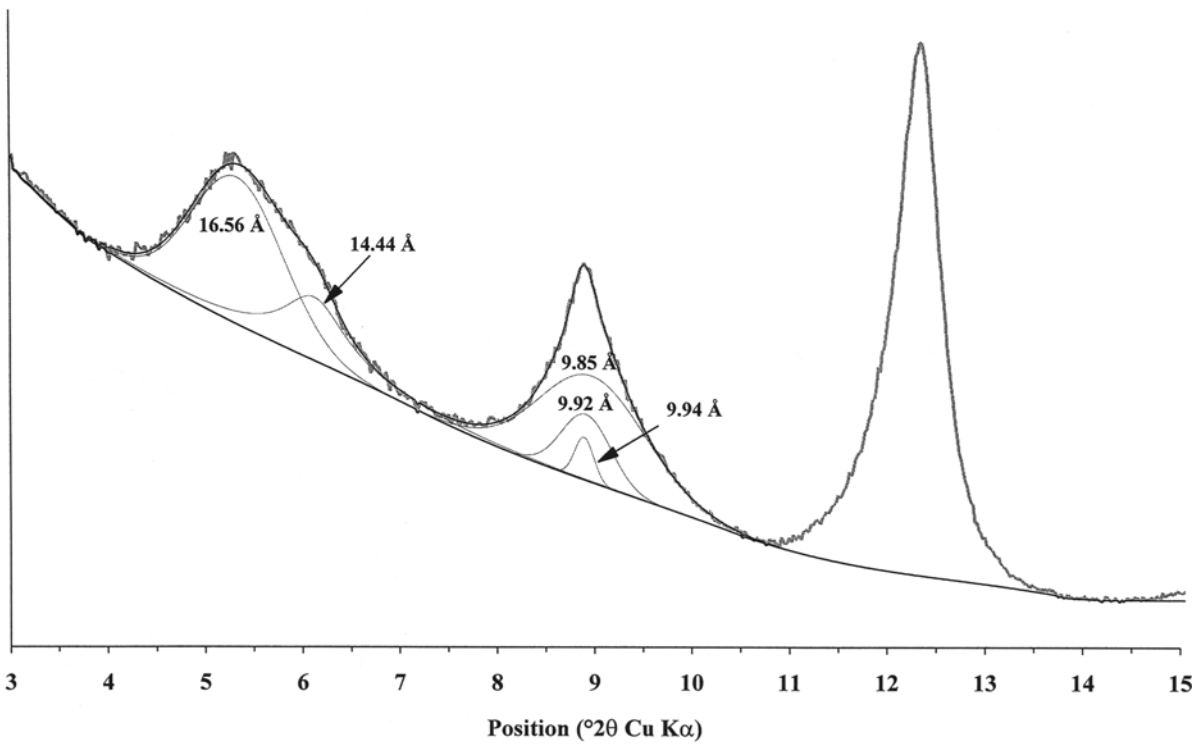


Figure 1a. Decomposition with 5 elementary peaks of the XRD pattern obtained from sample L353 (AD) after subtraction of a linearly interpolated background. These elementary peaks are associated with chlorite (14.46 Å), a randomly interstratified (R = 0) illite/smectite mixed layer (14.40 Å), an ordered (R = 1) I/S (11.33 Å), a low-CSDS illite (10.14 Å) and a high-CSDS micaceous phase (9.97 Å). Figure 1b. Decomposition with 5 elementary peaks of the XRD pattern obtained from sample L353 (EG) after subtraction of a linearly interpolated background. These elementary peaks may be associated with randomly interstratified (R = 0) illite/smectite mixed layer (16.56 Å), chlorite (14.44 Å), low-CSDS illite (9.92 Å) and high-CSDS micaceous phase (9.94 Å). The 002 peak related to the randomly interstratified I/S has not been found. Moreover, the 9.85-Å elementary peak, associated to an ordered (R = 1) I/S, has no counterpart in the 11–14 Å range (6.3–8.0 °2θ Cu$K\alpha$) because of inappropriate background subtraction.

https://doi.org/10.1346/CCMN.1997.0450202 Published online by Cambridge University Press

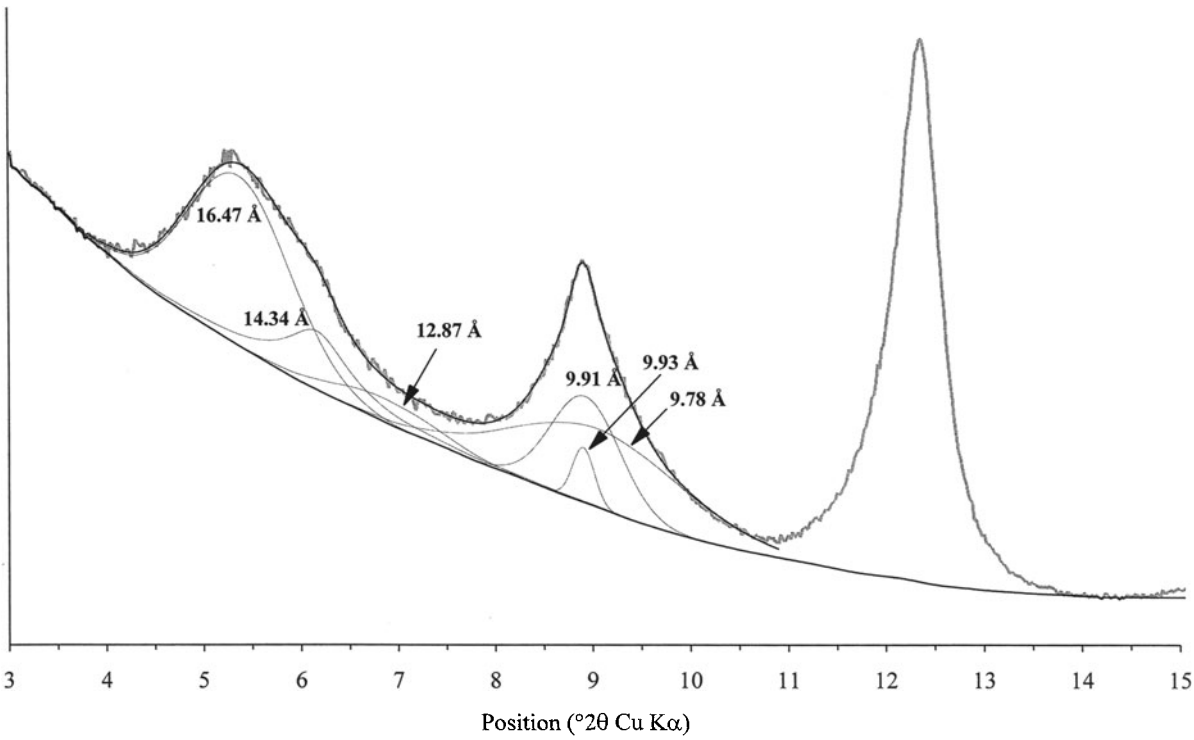


Figure 1c. Decomposition with 6 elementary peaks of the XRD pattern obtained from sample L353 (EG) after subtraction of a Lorentz factor-shaped interpolated background. These elementary peaks are associated with randomly interstratified (R = 0) I/S (16.47 Å), chlorite (14.34 Å), ordered (R = 1) I/S (12.87 Å and 9.78 Å), low-CSDS illite (9.91 Å) and a high-CSDS micaceous phase (9.93 Å). The 002 peak related to the randomly interstratified I/S has not been found. This identification is consistent with the one performed on the AD pattern of the same sample (Figure 1a).

step size must remain constant over the fitted angular range for convenience of calculation.

Additionally, data smoothing can be performed where experimental data seem too noisy to fit the profile directly. However, in such cases the sample can also be run again to obtain a more reliable data set, because both low peak/background ratio and statistical noise are prejudicial to a good decomposition (Howard and Preston 1989). Many data smoothing procedures, based mostly on a least-squares fitting to a parametric model, are detailed by Press et al. (1986). The solution used for DECOMPXR is to fit a third-degree polynomial over a window defined symmetrically on both sides of the considered point. The measured intensity is replaced by the value calculated using this polynomial expression, and the next point is then considered. Further details, numerical developments and examples are given by Lanson (1990). One should note that, if the window is too wide, the smoothing process can induce an alteration of the profile shape, especially on diffraction peak tails and tops.

Background Stripping

This step is necessary for DECOMPXR to fit the experimental profile, since the program assumes that the background is flat and null. However, it implies a loss of information from the sample. Both the Lorentz factor, which may include a preferred orientation function (Reynolds 1986), and the structure factor of the sample, which describes the scattering of the atoms from the elementary layers, contribute significantly to the "background", especially at low angles. The aim of eliminating the background before fitting is to reduce the total number of adjustable parameters as, most often, no information is extracted from the adjusted background. Furthermore, one should remember that this information is retrieved in the final step of the identification procedure when the experimental pattern is reconstructed from the simulated XRD profiles of the phases present in the sample.

Background stripping first requires the determination of experimental data points through which the background will be interpolated. The first point on the low-angle side of the pattern is assumed to belong to the background. To determine the next point, a line, initially vertical, is rotated counterclockwise around this point. When this line intersects the experimental profile, the rotation is stopped and the intersection point between the line and the pattern is assumed to belong to the background. This point is then used as

https://doi.org/10.1346/CCMN.1997.0450202 Published online by Cambridge University Press

rotation axis, and so on to the end of the pattern. This algorithm is detailed and illustrated by Lanson (1990). Such a procedure will only select data points on the lower experimental oscillations, that is, on the low limit of the intensity statistical domain (Liebhafsky et al. 1972):

$$[I_0 - \sqrt{I_0}; I_0 + \sqrt{I_0}] \quad [3]$$

where I_0 is the theoretical intensity without random fluctuation at this point.

In order to avoid systematic underestimation of the background, the intensity of these points is corrected before background interpolation. This correction is as follows (although it can be modified):

$$+\frac{\sqrt{I_0 - \sqrt{I_0}}}{2} \quad [4]$$

For reproducibility, it is recommended that linear interpolation be used in-between 2 data points defining the background when no additional constraints can be drawn. However, when the interpolation domain is very large (and thus, when the linear approximation is no longer valid), additional constraints are necessary. These constraints arise, for example, from differences between the results obtained from 2 XRD patterns of the same sample. Such a difference is illustrated in Figures 1a through 1c, where the ordered ($R = 1$) illite/smectite (I/S) 11.33-Å peak from the air-dried (AD) pattern (Figure 1a) has no correspondence in the 14–11-Å region of the ethylene glycol-solvated (EG) pattern (Figure 1b), when a linear background is interpolated. If the background is interpolated with a Lorentz factor-like shape (Figure 1c), an additional peak is needed to fit the experimental pattern. The positions of both this peak (12.87 Å) and of the one in the higher-angle region (9.78 Å) are compatible with the I/S phase. One can note also that the relative intensities of the various peaks are similar between both AD and EG patterns.

POTENTIAL EXPERIMENTAL LIMITATIONS

XRD Profile Symmetry of Single-Phase Samples

DECOMPXR uses symmetrical elementary peaks with either Gaussian or Lorentzian (Cauchy) shapes. To be valid, this approximation supposes that the diffraction peak of a single phase is symmetrical. If not, the various elementary peaks needed to fit the asymmetry have no physical meaning, because the contributions to this maximum are not summed up, but convoluted. Because the diffracted intensity is the product of the interference function (which is symmetrical) with the structure factor and the Lorentz-polarization factor (which are both strongly decreasing in the low-angle region; i.e., +2θ direction), diffraction peaks should be asymmetrical. Despite these theoretical restrictions, Lanson and Besson (1992) showed in the low-angle region (5–11 °2θ Cu$K\alpha$; 17.6–8.0 Å) and Lanson and Velde (1992) in the high-angle region (45.3 °2θ Cu$K\alpha$; 2.0 Å) that the diffraction peaks of a natural clay mineral (I/S) are symmetrical. These results were confirmed by Robinson and Bevins (1994) for the low-angle region of chlorite and chloritic mixed-layered XRD patterns.

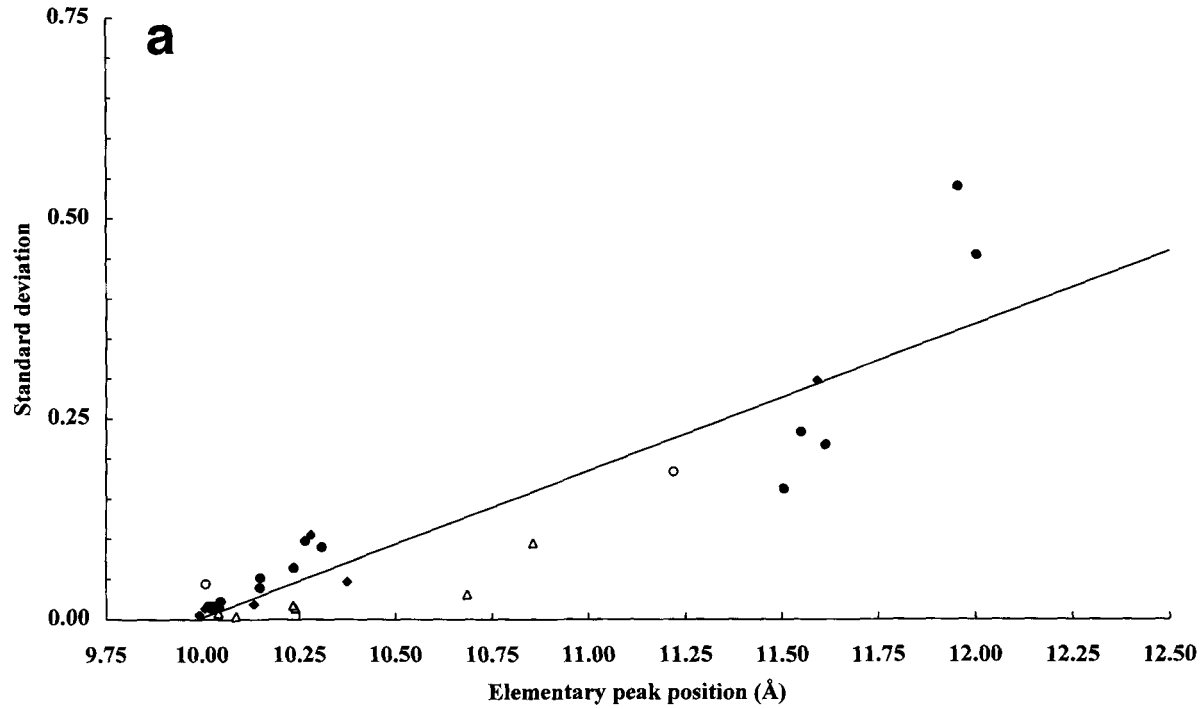
However, if the scatter of its physico-chemical characteristics (such as coherent scattering domain size, CSDS) is too large, the diffraction band of a single phase may be asymmetrical. In this case, the elementary peaks needed to fit the asymmetry are related to subpopulations of particles, which may be collectively considered to be a single phase. For example, the separation of 2 peaks, one associated with poorly crystallized illite and the other with a well-crystallized "mica", does not imply the actual existence of 2 distinct micaceous phases. If no detrital mica is present, both peaks may be related to the same authigenic illite phase, and are then a simplified way of describing a complex population of illite crystallites (Lanson and Velde 1992; Lanson et al. 1995). Even though such an asymmetric peak fit is artificial, various elementary peaks may be easier to interpret than an asymmetry coefficient. One should be careful not to interpret the existence of such a multiplet as evidence for a multiple-phase sample.

Experimental Reproducibility

DATA COLLECTION. To check the influence of sampling, sample preparation and data collection, Lanson (1990) performed 5 tests: 1) runs of the same slide with counting times ranging from 1 to 50 s per step; 2) repeated runs of the same slide with the same experimental conditions; 3) runs of several slides prepared from the same suspension; 4) runs of several slides prepared from samples from the same outcrop; and 5) runs of several slides prepared from cored samples from the same stratigraphic level (guided by γ-ray logs) in several wells from the same area (km scale). Details on these samples may be found in Lanson and Besson (1992). Their mineralogy is basically constant (mixture of illite and illitic I/S). Counting time has little influence on the profile shape, except for 1-s counting times, which are insufficient for reproducibility of results and which induce a slight peak broadening (Lanson 1990). For the other tests, a 3-s counting time was used. If long counting times are needed, it is better to collect several patterns with shorter counting times and to sum them, to avoid unmonitored variations of the intensity emitted by the tube.

Figure 2 shows the results of Tests 2 through 5. For each test, the greatest variability is shown by the material with the greatest expandabilities (highest peak position) and lowest CSDS (largest peak FWHM). Although the linear regressions shown are poorly correlated (R^2 equals 0.83 and 0.49, respectively, on Figures

https://doi.org/10.1346/CCMN.1997.0450202 Published online by Cambridge University Press



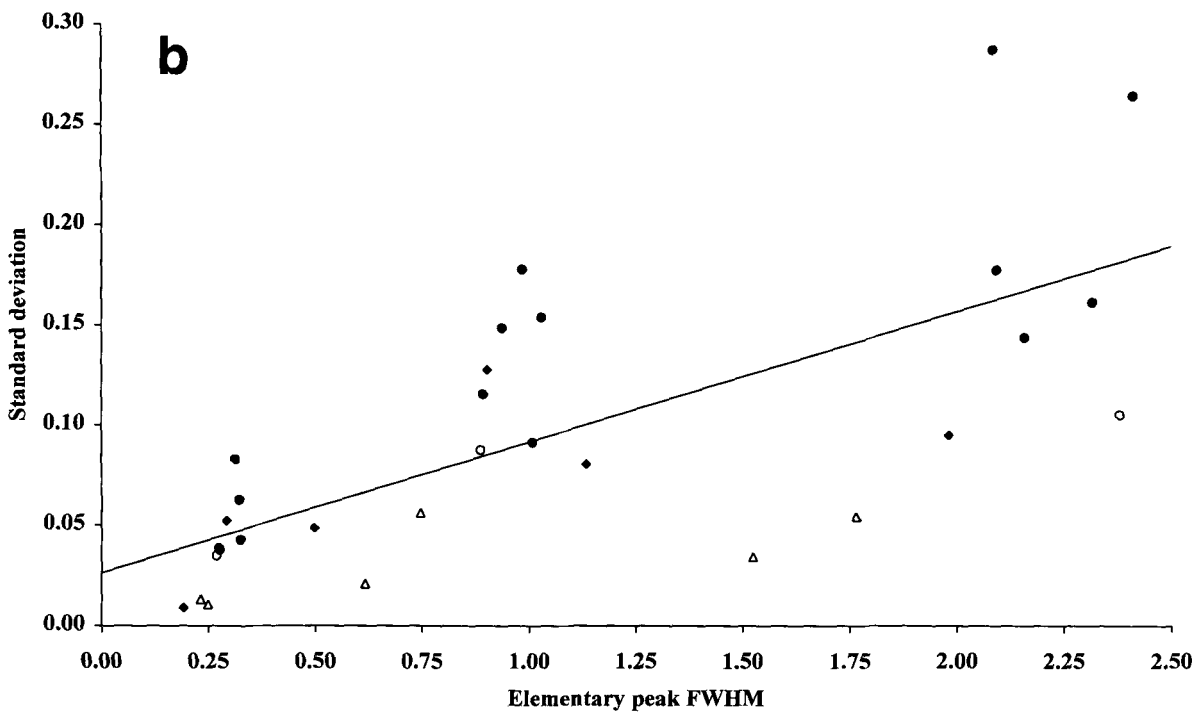


Figure 2a. Standard deviation on the determination of the elementary peak position as a function of the mean peak position for the various reproducibility tests performed (decomposition of AD patterns). Open triangles: various runs of the same slide (2 × 5 runs); solid diamonds: various slides from the same suspension (1 × 5 slides, 1 × 4 slides); open circles: various samples from the same outcrop (1 × 11 samples); solid circles: various samples from the same stratigraphic level (1 × 5 samples, 3 × 6 samples, 1 × 8 samples). R^2 equals 0.83 for the correlation line. Figure 2b. Standard deviation for the determination of the elementary peak FWHM as a function of the peak FWHM for the various reproducibility tests performed (decomposition of AD patterns). Patterns are as for Figure 2a. R^2 equals 0.49 for the correlation line.

https://doi.org/10.1346/CCMN.1997.0450202 Published online by Cambridge University Press

Table 1. Characterization of the DECOMPXR routine discrimination ability.

Characteristics of the elementary Gaussian profiles†§						Results of DECOMPXR best fit‡§					
Pos.	Int.	FWHM	Pos.	Int.	FWHM	Pos.	Int.	FWHM	Pos.	Int.	FWHM
8.00	500	1.10	8.80	500	0.60	8.00	500	1.10	8.80	500	0.60
8.50	500	0.85	8.80	500	0.60	8.50	500	0.85	8.80	500	0.60
8.60	500	0.80	8.80	500	0.60	*8.40*¶	*233*	*0.69*	*8.77*	*834*	*0.65*
8.70	500	0.75	8.80	500	0.60	*8.30*	*56*	*0.56*	*8.77*	*976*	*0.66*
8.80	500	0.70	8.80	500	0.60				*8.80*	*998*	*0.65*
8.50	100	0.85	8.80	500	0.60	8.50	100	0.85	8.80	500	0.60
8.60	100	0.80	8.80	500	0.60	*8.41*	*52*	*0.69*	*8.79*	*563*	*0.61*
8.60	500	0.80	8.80	100	0.60	*8.68*	*549*	*0.74*	*8.27*	*85*	*0.65*
8.70	500	0.75	8.80	500	0.40	8.70	500	0.75	8.80	500	0.40
8.70	500	0.70	8.80	500	0.40	*8.57*	*286*	*0.64*	*8.81*	*768*	*0.47*

† The characteristics (peak position, intensity and FWHM) of the 2 Gaussian profiles initially summed up are presented on the left side of the table.

‡ The decomposition results (see text for the logic of the decomposition process) are shown on the right side of the table.

§ Peak position and FWHM are expressed in °2θ, and the intensity in arbitrary units.

¶ When results differ from the original characteristics of the Gaussian profiles, they are displayed in italics.

2a and 2b), one can consider that the standard deviation is about the same for any test performed and depends mainly on the nature of the diffracting phase. The influence of sample preparation and alignment in the diffractometer cannot be distinguished from instrumental effects. Furthermore, as deduced from Tests 4 and 5, the inaccuracy induced by sample selection within a given sedimentary level is similar to the error of the decomposition method.

DECOMPOSITION PROCEDURE. To check the reproducibility of the decomposition procedure, the first step is to run the routine with different initial values and compare the results. This may seem obvious, but one would be surprised by the results from some commercially available routines. DECOMPXR fits the elementary peaks on the experimental data either with a least-squares method (Press et al. 1986) or with a nonlinear simplex method (Nelder and Mead 1965; Press et al. 1986). The convergence criteria used (±0.0005 °2θ Cu*K*α on any peak position or FWHM, ±0.5 counts on any peak intensity) guarantee the solution uniqueness for the least-squares method, even when initial values are defined very far from final results. When using the simplex method, the results depend slightly on the initial values (Howard and Snyder 1983). As a consequence, it should be run again to check for stable results. Usually, this method is used only when elementary peaks have characteristics too close to be fitted with a least-squares method, because of the similarities of their partial derivatives. In this case, the presence of these peaks can be assessed only if constraints are drawn from other XRD patterns. The estimation of initial values is usually sufficient to reduce the influence of this dependence on initial values. For example, on EG profiles, the least-squares method does not permit the separation of the I/S peak on the high-angle side of the 10-Å band and the peak associated with poorly crystallized illite (similar FWHM and difference of peak position ~0.3 °2θ Cu*K*α); but I/S and poorly crystallized illite are easily detected on the AD pattern.

When profile shape functions (PSF) more complex than Lorentz or Gauss profiles are used, the variation domain of the shape parameter can be interesting (e.g., the mixing parameter h for a pseudo-Voigt profile). Surprisingly, a pseudo-Voigt PSF (which is a linear combination of a Lorentz and a Cauchy profile) may not provide as good a fit as a single one of these elementary components (Stern et al. 1991).

Lanson and Velde (1992) also showed that the decomposition results are reliable whatever the program if the logical process followed to obtain the fit is unique. This uniqueness is important when results depend on initial values. However, their study showed that consistent results can be obtained from different diffraction systems and numerical processing programs.

Discrimination

Another important characteristic of a decomposition program is the ability to separate the respective contributions of various phases with similar characteristics and modify them as little as possible. From the decomposition of simulated XRD patterns and their sums, Lanson (1990) and Lanson and Besson (1992) indicated that it is possible to separate elementary peaks whose positions differ by 0.3 °2θ and their FWHM by 0.2 °2θ. To complement their study, elementary Gaussian profiles were calculated and summed up. The characteristics of these Gaussian profiles (Table 1) and the differences between their characteristics are similar to those observed in natural samples (Lanson and Champion 1991; Lanson and Velde 1992; Lanson et al. 1996). Sum profiles were fitted

https://doi.org/10.1346/CCMN.1997.0450202 Published online by Cambridge University Press

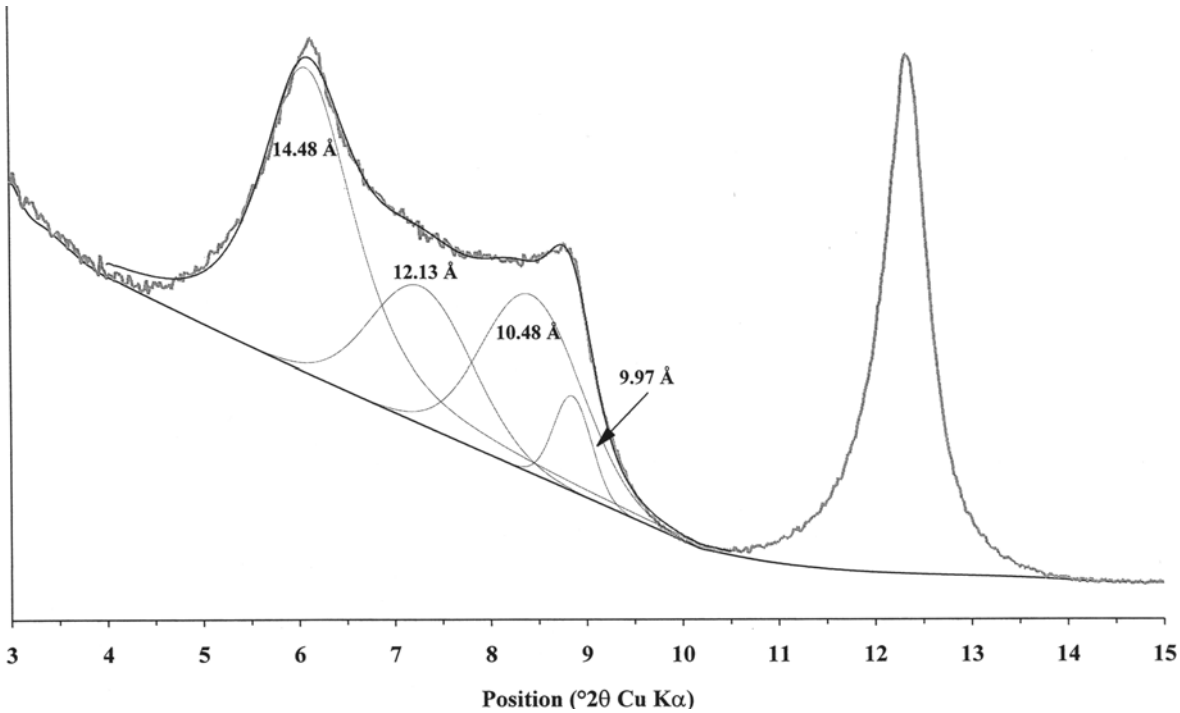


Figure 3. Decomposition with 4 elementary peaks of the XRD pattern obtained from sample L353 (AD) after subtraction of a linearly interpolated background. These elementary peaks are associated with a randomly interstratified (R = 0) illite/smectite mixed layer (14.48 Å), an ordered (R = 1) I/S (12.13 Å), a low-CSDS illite (10.48 Å) and a high-CSDS micaceous phase (9.97 Å). Even though not perfect, the fit could seem "acceptable"; however, the number of elementary peaks to be fitted is incorrect. The presence of a chlorite peak detected on the EG pattern of this sample (Figure 1c) explains the fit imperfection around 14.4 Å. Furthermore, the FWHM of the peak associated with the ordered I/S peak is inconsistent with the nature of this phase (see text for details).

first with a single elementary line. If some residual asymmetry was visible, an additional elementary peak was introduced, and the fitting routine was run again. From the results in Table 1, one can deduce that there is no alteration of the elementary contributions if their positions are separated by 0.30 and their widths by 0.25 °2θ. The relative proportions of the elementary components seem to have little, if any, influence on the discrimination threshold. This threshold may be lowered on 1 of the characteristics if the contrast on the other is enhanced. For example, it is possible to individualize elementary peaks whose positions differ only from 0.10 °2θ if their FWHM are separated by 0.35 °2θ. The overall discrimination threshold is lowered when the FWHM of the overlapping peaks are lower (for example, well-crystallized kaolinite 001 and chlorite 002).

DECOMPOSITION PROCEDURE

Method

The logical process followed to obtain the fit can influence the results if the calculation routine is imperfect. In the words of Howard and Preston (1989), "the subtleties involved in profile fitting commonly relegate the technique to the realm of art rather than science". Using DECOMPXR, speed and, in some tricky cases, reliability, may depend on the decomposition logic. Consequently, a standard procedure is proposed to lower the dependence of the results on the user: 1) collect the XRD profiles necessary for an unequivocal identification of clay phases (such as AD, EG or heated); 2) verify over the whole angular range, and between the profiles obtained from the same sample, the consistency of the identification; 3) verify that the theoretical pattern, which is the sum of all simulated patterns of phases identified in the sample, is similar to the experimental pattern over the whole angular range; 4) check for the existence and the nature of the phases detected by XRD profile decomposition with direct observations (for example, transmission electron microscopy—TEM—associated with chemical analyses, high-resolution TEM, atomic force microscopy).

DETERMINATION OF THE ANGULAR RANGE TO BE FITTED. The first step is to define the angular range to be fitted in such a way that the background intensity goes to zero or to a minimum (after background stripping) in order to get the best approximation possible of peak tails (for example, on the high-angle side of the 10-Å

https://doi.org/10.1346/CCMN.1997.0450202 Published online by Cambridge University Press

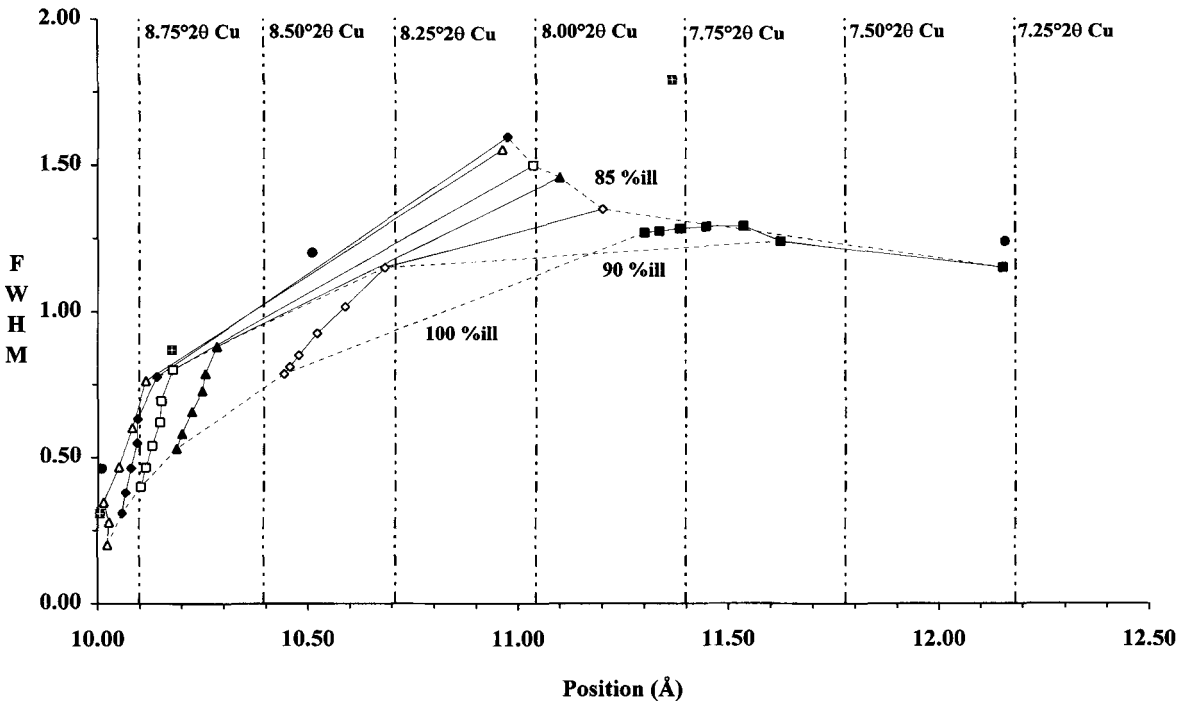


Figure 4. Identification diagrams for ordered (R = 1) mixed-layer illite/smectite, 001 illite/001 smectite peak. Peak widths (FWHM) are given in °2θ Cu$K\alpha$. Smectite layers are hydrated with 2 water layers, R = 1-ordering is maximum. The different patterns represent coherent scattering domain size (CSDS–thickness) distributions (solid squares $2 \leq N \leq 5$; empty diamonds $6 \leq N \leq 9$; solid triangles $11 \leq N \leq 14$; empty squares $16 \leq N \leq 19$; solid diamonds $22 \leq N \leq 25$; empty triangles: $36 \leq N \leq 39$). I/S composition varies from 85 to 100% illite (5% illite steps from 85 to 90% illite, and 2% illite increments from 90 to 100% illite). Dashed lines represent lines of iso illite content. If the characteristics of elementary peaks obtained from the decomposition procedure and attributed to ordered illitic I/S do not fall within this theoretically defined domain (or slightly above, see text), the preliminary identification must be rejected, and/or the number of elementary peaks defined again. Experimental decomposition results from Figure 1a (crosses) and from Figure 3 (solid circles) are plotted on the diagram.

band). An adequate angular range includes about ½ °2θ with minimum intensity on each side of the band of interest.

DETERMINATION OF THE NUMBER OF ELEMENTARY LINES TO BE FITTED. Because "the worst case is when the number of lines in a group is unknown" (Howard and Preston 1989), this step is essential for valid results. It will be detailed in 4 main stages:

1) Initial Determination of the Number of Elementary Peaks. Fit the experimental data with as few elementary contributions as possible, because the fit always improves as more parameters are fitted. The recommended procedure is to start fitting the band of interest with 1 elementary peak, and to increase the total number of these elementary contributions until an "acceptable" fit is obtained. This subjective condition is fulfilled when 3 conditions are satisfied: a) the general shape of the experimental diffraction band is reproduced; b) the sum of all fitted elementary contributions varies within the experimental noise; and c) the diffraction band tails are correctly modeled. On a complex band, this can be achieved either by directly fitting the complete angular range of interest or by first splitting this angular range in subranges. Both approaches give the same final results (Figure 3). The first process is faster, but the second is easier to master with little experience because fewer elementary peaks need to be defined at first, and thus fewer divergence problems are to be expected. These preliminary results are then checked; the consistency between peak position and FWHM is especially sensitive to an incorrect number of elementary peaks.

2) Constraints on Elementary Peak Characteristics from the Nature of Corresponding Phases. On Figure 3, these phases are illitic I/S or illite, except for the 14.48-Å peak. As a consequence, in an FWHM-versus-position plot, their parameters should fall within the theoretical domain defined (Lanson and Velde 1992) for simulated illite and illitic I/S (Figure 4), or possibly slightly above (Reynolds and Hower 1970; Lanson and Velde 1992). The inconsistently low FWHM (1.2 °2θ Cu$K\alpha$) of the 12.13-Å elementary peak indicates even more strongly than the slight misfit of the 14.5-Å maximum that the number of ele-

https://doi.org/10.1346/CCMN.1997.0450202 Published online by Cambridge University Press

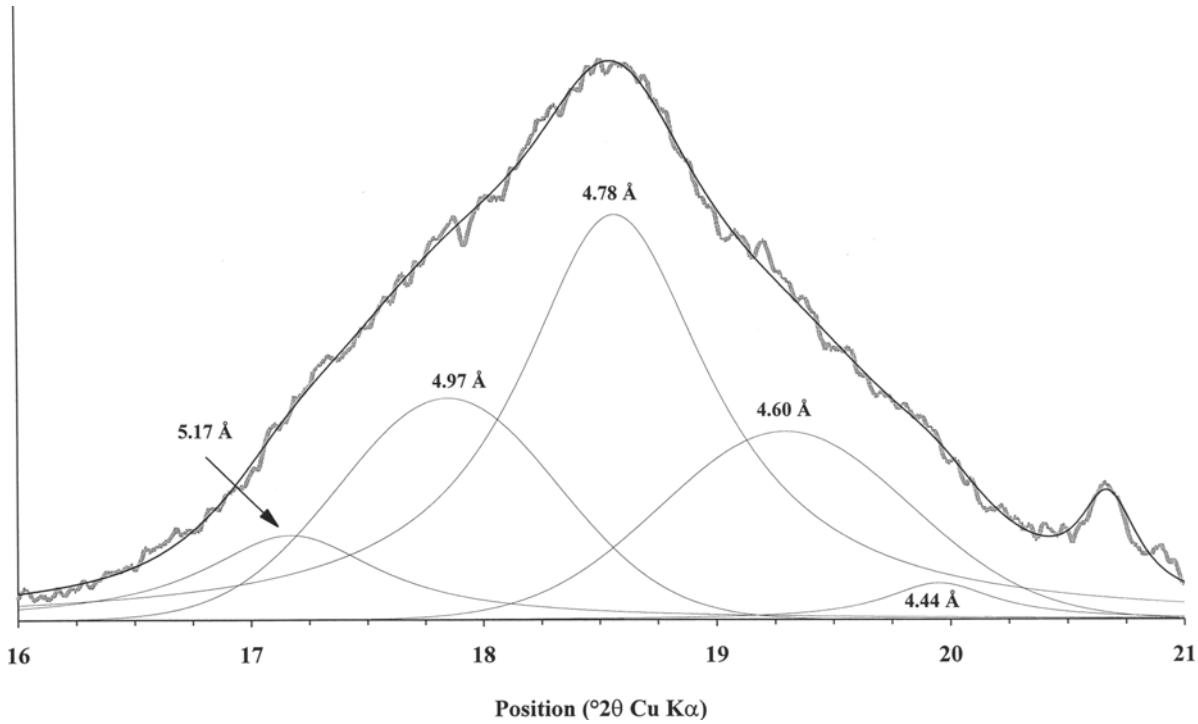


Figure 5. Decomposition with 5 elementary peaks of the XRD pattern obtained from sample SC1379 (EG) after subtraction of a linearly interpolated background. These elementary peaks are associated with domains of low-CSDS chlorite (4.78 Å), of corrensite (5.17 and 4.44 Å) and of a randomly interstratified (R = 0) 70:30 chlorite/corrensite mixed layer (4.97 and 4.60 Å).

mentary peaks fitted on this XRD profile is incorrect. Additionally, one must remember the basics of clay mineral identification when using the decomposition procedure. The XRD peaks of mica and chlorite must be located at 10.0 and ~14.2 Å, respectively. Furthermore, illite is a nonexpandable phase, and the associated elementary peaks (usually 2 in samples of diagenetic origin) must not shift with EG solvation.

3) Constraints on the Number of Elementary Peaks from Additional XRD Patterns. A careful examination for consistency is essential for the indisputability of the decomposition results, and it must take into account all of the diffraction patterns recorded for the sample. For the above example, compare Figure 1a (sample L353 fitted with 5 elementary peaks) to Figure 3 (sample L353 fitted with 4 elementary peaks). The final proof of the need for an additional elementary peak is given by the presence of a chlorite peak on the EG pattern (Figure 1c). One must be aware that the aim of the decomposition procedure is not to perform a complete characterization of a sample from the processing of a single band. The decomposition method is not intended, and is not able, to substitute for the various treatments used to characterize clay minerals, such as solvation with a polar organic molecule (ethylene glycol or glycerol), heating or other treatments common in soil science. Examples of the latter are K-saturation followed by heating to 110, 300 and 550 °C; Li-saturation and heating to 300 °C; and high-gradient magnetic separation. The aim of this method is to provide more information from an XRD profile.

4) Constraints on the Number of Elementary Peaks from the Decomposition of High-Angle XRD Bands. In the region 15–50 °2θ Cu$K\alpha$ (5.9–1.8 Å), the influence of the CSDS on peak position diminishes (Reynolds and Hower 1970; Środoń 1980; Reynolds 1989). Thus, though possible, the differentiation between particle (sub-)populations with identical crystallo-chemical structure (pure illite) and wide crystallinity range (i.e., CSDS) is much more complex to perform on higher-angle ranges. The maxima associated with the various (sub-)populations display identical positions and can frequently be fitted globally with a unique PSF, including a shape parameter (for example, pseudo-Voigt or Pearson 7; Lanson and Velde 1992). However, the agreement is good between CSDS and composition (illite content) obtained from the analysis of various angular ranges (Lanson and Velde 1992, Table 3).

Finally, the comparison with data derived from direct observations (such as TEM) or from other methods (such as chemical analyses) constitutes an essential part of the check for results consistency.

Verifying the choice of the number of elementary peaks is time-consuming and may seem to eliminate

https://doi.org/10.1346/CCMN.1997.0450202 Published online by Cambridge University Press

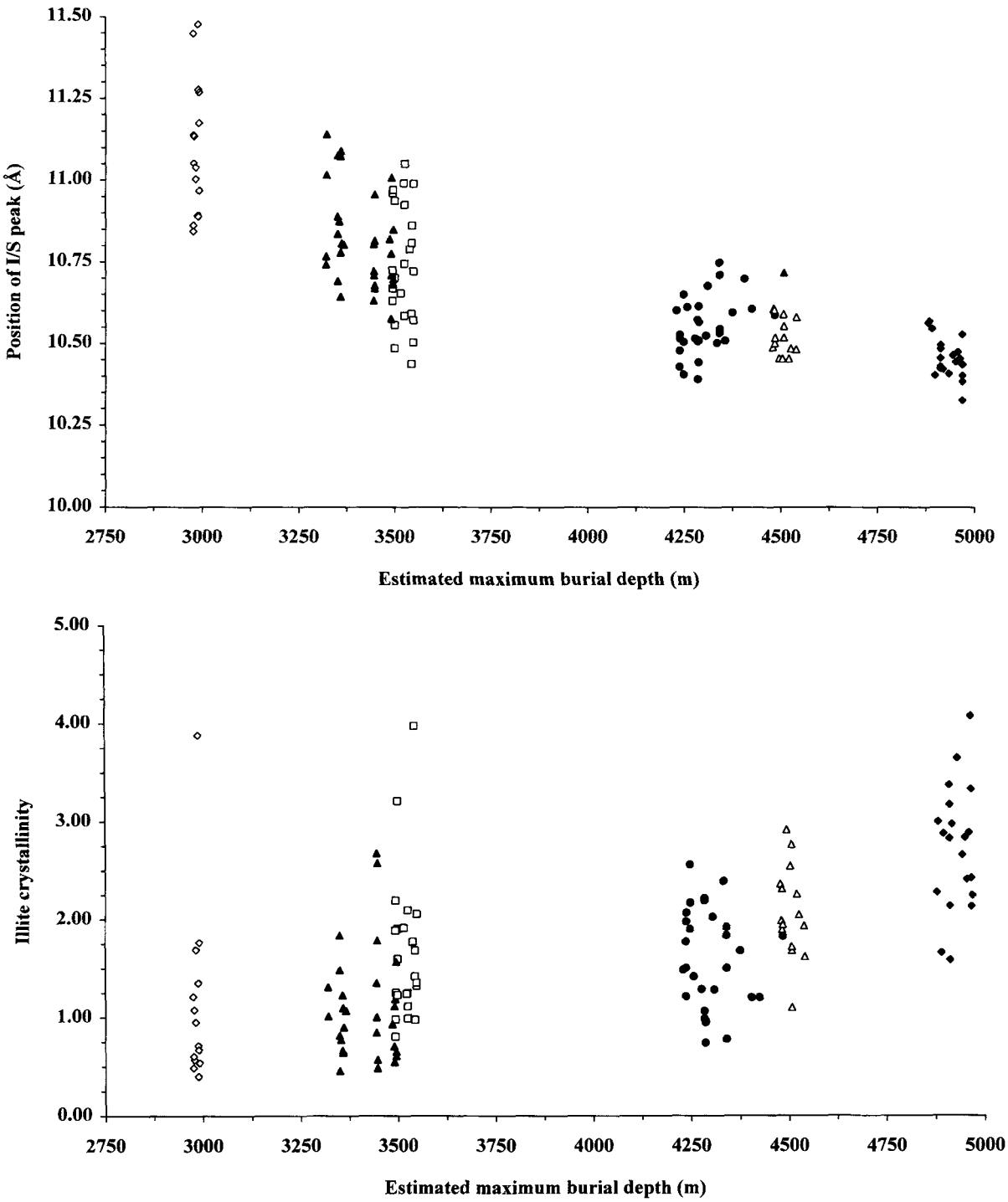


Figure 6a. Evolution of the ordered I/S peak position, obtained from peak decomposition of AD samples, as a function of estimated maximum burial depth (modified from Lanson et al. 1995). Samples are clay fraction (< 5.0 μm to < 0.2 μm) from the Rotliegend Sandstone Reservoir in the Broad Fourteens Basin, Dutch sector, southern North Sea. Patterns represent various wells within a single graben (open diamonds: well 1; solid triangles: well 2; open squares: well 6; solid circles: well 3; open triangles: well 4; solid diamonds: well 5). Figure 6b. Evolution of illite crystallinity as a function of the estimated maximum burial depth (modified from Lanson et al. 1995). Samples and patterns as for Figure 6a. The crystallinity index (CI) is expressed as:

$$0.1/[\text{PCI peak rel int} \times \text{PCI peak FWHM} \times (\text{PCI peak pos} - \text{WCI peak pos})] \quad [5]$$

https://doi.org/10.1346/CCMN.1997.0450202 Published online by Cambridge University Press

one of the main advantages of the decomposition method; that is, its ability to quickly and accurately characterize a great number of samples. However, the clay mineral identification can be trusted only when it results from the analysis of all diffraction bands collected from the sample of interest. When working on a continuous series of samples (such as a diagenetic series down a borehole), the checks for consistency can be restricted to a limited number of samples selected throughout the series. The validated results are then used as starting values for the decomposition of all other samples over a restricted diagnostic angular range, speeding characterization.

PROFILE SHAPE OF ELEMENTARY PEAK. So far, this parameter has not been studied systematically for clay minerals. In a preliminary study using a PSF with an adjustable shape parameter, Lanson and Velde (1992) showed that the decomposition results obtained using either a Pearson 7 or a Gaussian PSF are very similar, at least for illite-I/S-chlorite mixtures, and that the choice of the PSF does not influence the decomposition results. They also indicated that diffraction maxima of single phase I/S are almost ideally Gaussian, despite contrary statements in the literature (Howard and Preston 1989; Stern et al. 1991). Better-crystallized clay minerals such as chlorite or a mica-like phase are shown to be Lorentzian-shaped peaks. The origin of these different peak shapes is unknown. These results may be compared with the Gaussian profile used to describe the strain broadening or the Lorentzian profile used to describe the broadening due to small crystallite size and size distributions (Klug and Alexander 1974; Louër and Langford 1988).

Prospects

PHYSICAL MEANING. As shown above (Figure 3), one has to be extremely careful about the physical meaning of the decomposition results. The decomposition procedure is just a numerical routine and the check for results validity is the user's responsibility. The above example (Figures 1 and 3) illustrates the necessary consistency between peak position and FWHM, which are dependent for a given phase. An additional constraint on peak FWHM is the lower limit defined by the instrumental width (approximately 0.05 °2θ in the best case). This constraint may be a problem only for very well-crystallized phases such as kaolinite, dickite (Lanson et al. 1996) or chlorite. In such cases, the instrumental contribution to the experimental profile cannot be neglected and the pure diffraction profile has to be deconvoluted before any further analysis.

Furthermore, the decomposition procedure is theoretically justified only if separate phases are actually present in the sample or if different peaks from the same phase are overlapping (e.g., ordered I/S after EG solvation). From position, FWHM and relative intensities of the elementary peaks representing a phase (which is actually a population of particles with variable characteristics), the mean value of some physicochemical characteristics (such as composition and CSDS) is derived. When the scatter of these characteristics is limited, experimental diffraction peaks of single-phase clay mineral samples are symmetrical. If the dispersion of these characteristics is large enough, it may induce distinguishable diffraction "peaks" for a single population/phase. The use of several elementary peaks to characterize a single phase must be supported by evidence from additional analyses (such as scatter of individual particle composition or scatter of the particle size and thickness). This case is common in late-stage diagenesis; for example, where illitic I/S coexists with pure illite having very variable CSDS (Lanson and Champion 1991; Lanson and Velde 1992; Renac and Meunier 1995; Varajao and Meunier 1995; Lanson and Meunier 1995; Lanson et al. 1996). In this case, the CSDS distribution is usually fitted with 2 distinct elementary peaks related to "poorly crystallized" and "well-crystallized" illites (Lanson and Meunier 1995). However, both peaks represent 1 phase, and their evolution must be interpreted in terms of CSDS distribution for the whole illite crystal population.

RELEVANCE AND APPLICATIONS. The application of such a decomposition method is not restricted to multiple-phase samples, but can also help to quickly and accurately identify a single phase. In addition to the position of the diffraction maxima, even overlapping ones in the case of mixed-layered minerals, the decomposition procedure also provides their FWHM and relative intensity. These additional constraints can

---

←

where:

$$\text{PCI peak rel int} = \frac{\text{PCI int}}{\text{PCI int} + \text{WCI int} + I - S \text{ int}}. \quad [6]$$

The relative intensity of the PCI peak is expressed in %. Peak positions are expressed in Å, whereas FWHM is expressed in °2θ Cu$K\alpha$. The differentiation between PCI and WCI is simply a convenient way to describe the illite population, but does not imply the actual existence of 2 populations of illite particles (Lanson and Meunier 1995). This index accounts for the relative proportion of illite crystallites with low CSDS. Furthermore, the CSDS of these poorly crystallized particles is accounted for by the influence of low CSDS values both on peak position (shift towards low angle) and on peak FWHM (peak broadening).

https://doi.org/10.1346/CCMN.1997.0450202 Published online by Cambridge University Press

more precisely define the crystallo-chemical structure of the single phase.

The decomposition method is especially suited for the characterization of complex clay assemblages. Such mixtures have been described in late-stage diagenesis (Figure 1a and 1c; Lanson and Champion 1991; Lanson and Besson 1992; Matthews et al. 1994; Lanson et al. 1995; Renac and Meunier 1995; Varajao and Meunier 1995; Lanson et al. 1996), soils (Righi and Meunier 1991; Righi et al. 1993; Righi et al. 1995), experimental hydrothermal alteration of clay minerals (Bouchet et al. 1992) and hydrothermal systems (Robinson and Bevins 1994). In Figure 5, the diagnostic 16–21 °2θ Cu*K*α range (5.55–4.25 Å, Moore and Reynolds 1989) for chloritic mixed layers of sample SC1379 is fitted with 5 elementary peaks. These peaks indicate the coexistence of corrensite (5.17 and 4.44 Å), chlorite (4.78 Å), and $R = 0$ chlorite/corrensite mixed-layer (4.97 and 4.60 Å) scattering domains. These domains can be interpreted either as separate individual phases or as a more complex chlorite/corrensite $R = 1$ segregated mixed layer.

Finally, the ability of DECOMPXR to describe variations affecting the characteristics (such as CSDS or composition) of a series of samples is illustrated by the decomposition of the 10-Å band of illitic materials (Figure 6). It yields information not only on illite "crystallinity" but also on the composition (smectite content) of the I/S phase and possibly on the relative proportions of both phases (Lanson et al. 1995, Figure 12). This complete characterization of the illitic material allows extensive comparisons, the structure of these minerals being used as a correlation probe for burial paleo-conditions (Lanson et al. 1995, 1996) or stratigraphy. Furthermore, the precise description of the structural state of illitic material throughout a diagenetic series is essential to determining the reaction mechanisms of the smectite-to-illite diagenetic transformation.

CONCLUDING REMARKS

The decomposition procedure (such as DECOMPXR) is easy and fast to perform, and can be used as a descriptive tool on a great number of samples. Results accuracy is mostly a function of data collection reproducibility and is not much affected by numerical processing, except for the background stripping that may induce a slight modification of the peak profile. This profile is symmetrical for a single-phase clay mineral except when the scatter is too large because of its physico-chemical characteristics (such as CSDS). In this case, the elementary peaks needed to fit the asymmetry are related to subpopulations of particles, which can be considered a single phase. The resolution of the routine permits fitting elementary peaks whose positions differ from 0.30 °2θ and their FWHM from 0.25 °2θ. Lower discrimination thresholds may be reached on 1 characteristic (position or FWHM) if the difference on the other is enhanced. The overall discrimination threshold is lower when the FWHM of the overlapping peaks is less than 0.6 °2θ. In conclusion, the minor experimental limitations (for additional details, see Lanson 1990) make this method a powerful and reliable tool to describe XRD patterns of clay mineral mixtures.

Because of the verifications necessary to validate the results, decomposition is especially suited to study sample series, and, in particular, to describe variations affecting their components. In the case of isolated samples, the decomposition procedure provides the user with peak parameters for any detectable phase. This information is especially useful for complex clay mineral assemblages.

The proposed verifications (over the whole angular range, between the various profiles and against analytical results from other methods) allow the decomposition method to be used not only as a descriptive tool, but also as an identification method for the clay minerals coexisting in complex assemblages. Additional parameters (such as the FWHM) provided by the decomposition analysis are essential for the identification of these phases, because they represent additional constraints for the simulation of their XRD profiles. XRD pattern simulation is usually constrained from the analysis of a restricted angular range. However, the ultimate identification is to be confirmed by comparison over the whole angular range of both the experimental and the simulated patterns.

The accuracy of peak characteristics provided by the decomposition method allows one to confirm that the theoretical description of I/S mixed layers used for the simulation is slightly incorrect. The well-known mismatches of peak width observed in the 5–11 °2θ Cu*K*α (17.6–8.0 Å) range (Reynolds and Hower 1970; Środoń 1980; Reynolds 1980; Lanson and Champion 1991; Lanson and Velde 1992), as well as the gap between experimental and theoretical position-FWHM values in the 17.7 °2θ Cu*K*α (5.00 Å) region (Lanson and Velde 1992) illustrate these defects for I/S mixed layers. A more realistic structural model includes the variation from the average structure and the presence of defects that affect their reactivity and growth. The presence of incomplete layers within the stacking sequence (Pevear et al. 1991; Tsipursky et al. 1992), the coexistence of various hydration states (Pons et al. 1981 and 1982) or the scatter of elementary layer thicknesses around a mean value (Kodama et al. 1971; Środoń 1980; Sato et al. 1992) are some of the defects and strains that can modify XRD line profiles.

The decomposition procedure is useful not only to describe trends, but also to identify the various phases present throughout series of samples. This is the first step to constrain and determine the reaction mechanisms of a transformation and, as a consequence, to

https://doi.org/10.1346/CCMN.1997.0450202 Published online by Cambridge University Press

characterize and model the kinetics of this transformation. Furthermore, a detailed description of clay mineral population seems necessary for determining the relationships between structure and chemical properties (reactivity) on the one hand and between structure and physical properties (shape, induced roughness of porosity, impact on permeability) on the other. Furthermore, it must be remembered that the effect of structure on clay mineral growth is induced not only by the 1-dimensional arrangement of these minerals but, predominantly, by their 3-dimensional structure, whose determination may also be enhanced by the decomposition procedure.

ACKNOWLEDGMENTS

The author thanks D. Beaufort, S. Hillier, A. Meunier, D. Righi and B. Velde for corrections and comments on early versions of the manuscript, and acknowledges financial support from EAP (Géochimie Minérale laboratory, Pau). The manuscript greatly benefited from the reviews of D.M. Moore and J. Środoń.

REFERENCES

Bouchet A, Lajudie A, Rassineux F, Meunier A, Atabek R. 1992. Mineralogy and kinetics of alteration of a mixed-layer kaolinite/smectite in nuclear waste disposal simulation experiment (Stripa site, Sweden). Appl Clay Sci 7: 113–123.

Drits VA, Tchoubar C, Besson G, Bookin AS, Rousseaux F, Sakharov BA, Tchoubar D. 1990. X-ray diffraction by disordered lamellar structures: theory and applications to microdivided silicates and carbons. Berlin: Springer-Verlag. 371 p.

Drits VA, Weber F, Salyn AL, Tsipursky SI. 1993. X-ray identification of one-layer illite varieties: application to the study of illites around uranium deposits of Canada. Clays Clay Miner 41:389–398.

Howard SA, Preston KD. 1989. Profile fitting of powder diffraction patterns. In: Bish DL, Post JE, editors. Reviews in mineralogy 20: Modern powder diffraction. Washington, DC: Miner Soc Am. p 217–275.

Howard SA, Snyder RL. 1983. An evaluation of some profile models and optimization procedures used in the profile fitting. Adv X-ray Anal 26:73–81.

Jones RC. 1989. A computer technique for X-ray diffraction curve fitting/peak decomposition. In: Pevear DR, Mumpton FA, editors. Clay Minerals Society workshop lectures, vol 1: Quantitative mineral analysis of clays. Boulder, CO: Clay Miner Soc. p 51–101.

Klug HP, Alexander LE. 1974. X-ray diffraction procedures for polycrystalline and amorphous materials. New York: J Wiley. 966 p.

Kodama H, Gatineau L, Méring J. 1971. An analysis of X-ray diffraction line profiles of microcrystalline muscovites. Clays Clay Miner 19:405–413.

Lanson B. 1990. Mise en évidence des mécanismes de transformation des interstratifiés illite/smectite au cours de la diagenèse [Ph.D. thesis]. Paris: Univ. Paris 6 - Jussieu. 366 p.

Lanson B, Beaufort D, Berger G, Baradat J, Lacharpagne JC. 1996. Late-stage diagenesis of clay minerals in porous rocks: Lower Permian Rotliegendes reservoir off-shore of The Netherlands. J Sed Res 66:501–518.

Lanson B, Beaufort D, Berger G, Petit S, Lacharpagne JC. 1995. Evolution de la structure cristallographique des minéraux argileux dans le réservoir gréseux Rotliegend des Pays-Bas. Bull Cent Rech EAP 19:243–265.

Lanson B, Besson G. 1992. Characterization of the end of smectite-to-illite transformation: Decomposition of X-ray patterns. Clays Clay Miner 40:40–52.

Lanson B, Champion D. 1991. The I/S-to-illite reaction in the late stage diagenesis. Am J Sci 291:473–506.

Lanson B, Meunier A. 1995. La transformation des interstratifiés ordonnés (S ≥ 1) illite/smectite en illite dans les séries diagénétiques: état des connaissances et perspectives. Bull Cent Rech EAP 19:149–165.

Lanson B, Velde B. 1992. Decomposition of X-ray diffraction patterns: a convenient way to describe complex diagenetic smectite-to-illite evolution. Clays Clay Miner 40: 629–643.

Liebhafsky HA, Pfeiffer HG, Winslow EH, Zemany PD. 1972. X-rays, electrons, and analytical chemistry: Spectrochemical analysis with X-rays. New York: J Wiley. 566 p.

Louër D, Langford JI. 1988. Peak shape and resolution in conventional diffractometry with monochromatic X-rays. J Appl Crystallogr 21:430–437.

Matthews J, Velde B, Johansen H. 1994. Significance of K-Ar ages of authigenic illitic clay minerals in sandstones and shales from the North Sea. Clay Miner 29:379–389.

Moore DM, Reynolds RC, Jr. 1989. X-ray diffraction and the identification and analysis of clay minerals. Oxford: Oxford Univ Pr. 322 p.

Nelder JA, Mead R. 1965. A simplex method for function minimization. Computer J 7:757–769.

Pevear DR, Klimentidis RE, Robinson GA. 1991. Genetic significance of kaolinite nucleation and growth on pre-existing mica in sandstones and shales. In: Program and abstracts for the Clay Miner Soc 28th annual meeting; Houston, Texas. p 125.

Pons CH, Rousseaux F, Tchoubar D. 1981. Utilisation du rayonnement synchrotron en diffusion aux petits angles pour l'étude du gonflement des smectites: I. Etude du système eau-montmorillonite-Na en fonction de la température. Clay Miner 16:23–42.

Pons CH, Rousseaux F, Tchoubar D. 1982. Utilisation du rayonnement synchrotron en diffusion aux petits angles pour l'étude du gonflement des smectites: II. Etude de différents systèmes eau-smectites en fonction de la température. Clay Miner 17:327–338.

Press WH, Flannery BP, Teukolsky SA, Vetterling WT. 1986. Numerical recipies: The art of scientific computing. Cambridge: Cambridge Univ Pr. 818 p.

Renac C, Meunier A. 1995. Reconstruction of paleothermal conditions in a passive margin using illite/smectite mixed-layered series (BA1 scientific deep drill-hole, Ardèche, France). Clay Miner 30:107–118.

Reynolds RC Jr. 1980. Interstratified clay minerals. In: Brindley GW, Brown G, editors. Crystal structures of clay minerals and their X-ray identification. London: Miner Soc. p 249–359.

Reynolds RC Jr. 1986. The Lorentz-polarization factor and preferred orientation in oriented clay aggregates. Clays Clay Miner 34:359–367.

Reynolds RC Jr. 1989. Diffraction by small and disordered crystals. In: Bish DL, Post JE, editors. Reviews in mineralogy 20: Modern powder diffraction. Washington, DC: Miner Soc Am. p 145–181.

Reynolds RC Jr, Hower J. 1970. The nature of interlayering in mixed-layer illite-montmorillonites. Clays Clay Miner 18:25–36.

Righi D, Meunier A. 1991. Characterization and genetic interpretation of clays in an acid brown soil (dystrochrept) developed in a granitic saprolite. Clays Clay Miner 39: 519–530.

Righi D, Petit S, Bouchet A. 1993. Characterization of hydroxy-interlayered vermiculite and illite/smectite interstra-

https://doi.org/10.1346/CCMN.1997.0450202 Published online by Cambridge University Press

tified minerals from the weathering of chlorite in a cryothod. Clays Clay Miner 41:484–495.
Righi D, Velde B, Meunier A. 1995. Clay stability in clay-dominated soil systems. Clay Miner 30:45–54.
Robinson D, Bevins RE. 1994. Mafic phyllosilicates in low-grade metabasites. Characterization using deconvolution analysis. Clay Miner 29:223–237.
Sato T, Watanabe T, Otsuka R. 1992. Effects of layer charge, charge location, and energy change on expansion properties of dioctahedral smectites. Clays Clay Miner 40:103–113.
Środoń J. 1980. Precise identification of illite/smectite interstratifications by X-ray powder diffraction. Clays Clay Miner 28:401–411.
Stern WB, Mullis J, Rahn M, Frey M. 1991. Deconvolution of the first "illite" basal reflection. Schweiz Mineral Petrogr Mitt 71:453–462.
Tsipursky SJ, Eberl DD, Buseck PR. 1992. Unusual tops (bottoms?) of particles of 1M illite from the Silverton caldera (CO). In: Agronomy abstracts annual meetings. Madison, WI: Am Soc Agron. p 381–382.
Varajao A, Meunier A. 1995. Particle morphological evolution during the conversion of I/S to illite in lower cretaceous shales from Sergipe-Alagoas Basin, Brazil. Clays Clay Miner 43:14–28.

(Received 8 August 1995; accepted 22 April 1996; Ms. 2679)

https://doi.org/10.1346/CCMN.1997.0450202 Published online by Cambridge University Press